The Role of Radar Cross-Section in Advanced Aircraft Stealth Design

Samuel Lee*

Wardlaw-Hartridge School, Edison, United States

* Corresponding Author Email: minecapy123@gmail.com

Abstract. This paper aims to give an introduction into the radar cross-section of objects. Specifically, it goes into the importance that the radar cross-section has on the design of stealth aircraft. It provides the importance of the radar cross-section in the construction of stealth aircraft and why it is such an important factor, outlines the definition of radar cross-section, and describes multiple methods of calculating it. This paper will cover three methods of calculating radar cross-section, being Geometric Optics, Physical Optics and the Method of Moments. It details how the methods function, what they should be used for when calculating radar cross-section of aircraft, and steps and formulas that will solve the RCS of the target object. Finally, it gives an insight into the future design direction of sixth-generation stealth aircraft, what a future sixth-gen fighter would have compared to the current fifth-generation fighters of today, and other fields where radar stealth is an important factor, such as the creation of stealth warships.

Keywords: Radar Cross-Section, Aircraft, Stealth Design.

1. Introduction

The radar cross-section (RCS) of an object is the measure of how easily an object is detected by radar. The smaller the radar cross-section, the less likely it is to be detected by radar. More specifically, it is the ability of an object to capture the incident radar wave and scatter it back to the receiver [1]. While every object possesses a radar cross-section, it is most important when pertaining to military vehicles, with an extra focus on aircraft, both unmanned and manned. An aircraft with a low radar cross-section is classified as a low-observable (LO) or, more commonly, a "stealth" aircraft. Stealth aircraft rose into prominence as military doctrine shifted from the dogfights of World War II and the Korean War to beyond-visual-range (BVR) combat, which sprouted its roots in the jungles of Vietnam but really only came into fashion during the Gulf War in 1991. Beginning with the testbed of the first stealth aircraft, the Have Blue, as seen in Fig. 1, engineers across the planet have built increasingly stealthier designs over the years. With aircraft radar becoming more advanced and the ever-increasing range of air-to-air (AAM) and surface-to-air (SAM) missiles, fifth-generation (F-22, F-35, J-20, Su-57) and future sixth-generation (NGAD, F/A-XX, PAK DP) aircraft designs all feature a reduction of the radar cross-section as a major aspect of their construction. RCS is measured usually in meters squared or dBsm (decibels relative to a square meter), with most modern stealth aircraft having at least an RCS of less than 0.0002m^2 [2], though this figure can likely be reduced even further, with the advent of modern technologies. dBsm and m^2 are interchangeable by the equation of

$$RCS_{dBsm} = 10 \log_{10} RCS_{m^{\wedge}2} \quad (1)$$

where the dBsm RCS can be derived from the m^2 version [1].

To understand how a small radar cross-section affects the detectability of an aircraft, it is important to understand how modern radars work when pertaining to aircraft. A radar works by firing radio waves at a given region, then receives any waves that have bounced back via hitting any object. With this, it can then calculate where an object is and then provide coordinates and distance. However, to reduce clutter, filters are put in place to disregard certain returns, such as very small signatures made by birds, and any waves returning from a low altitude to disregard objects such as trees. It is these filters that help a small radar cross-section stay undetected as they will likely be filtered out, and it is

the same reason aircraft will fly at very low altitudes, literally "under the radar", to avoid detection. Additionally, a small radar-cross section means that some radio waves will simply never make it back to the receiver in the first place, either being absorbed or reflected away from the receiver.

Fig. 1 The Lockheed Have Blue prototype undergoing RCS testing in an anechoic chamber

Therefore, it is incredibly obvious that RCS is an important aspect of stealth aircraft construction and a major focus of future combat aircraft. It is no coincidence that many fifth-generation designs look relatively similar, as certain design aspects simply just work the best in reducing detection. Features such as a flush body, V-tail and internal weapon bays are all hallmarks of fifth-generation designs. With the introduction of the B-2 stealth bomber, lessons learned from that design, such as a complete removal of the horizontal stabilizer, is also being incorporated into future sixth-generation designs along with the aforementioned features. With the air war becoming increasing longer ranged, stealth designs are now almost essential for the survival of future aircraft.

2. Literature Review

As stated already, the RCS of an aircraft is a major aspect of stealth aircraft design. A smaller RCS means increased difficulty to be locked on by radars, whether that be from SAM sites or radar-guided AAMs from enemy fighter aircraft, such as the AIM-120 or R-77. Additionally, being harder to detect gives the aircraft an edge in BVR engagements, provided both sides possess similar radar ranges. In the current age of aerial warfare, being able to detect the enemy aircraft first provides a massive advantage, since the detecting aircraft can launch their missiles first, unless limited by missile range.

The radar cross-section can be defined by the equation

$$\sigma = \lim_{R\to\infty} 4\pi R^2 \frac{|E_{scattered}|^2}{|E_{incident}|^2} \tag{2}$$

where R = distance from the radar, $E_{scattered}$ is the scattered electric field intensity returning to the radar, $E_{incident}$ is the electric field intensity incident on the target, and σ being the RCS [1][3]. Another version of the equation can be written using power density, being

$$\sigma = \lim_{R\to\infty} 4\pi R^2 \frac{P_{scattered}}{P_{incident}} \tag{3}$$

where $P_{scattered}$ is the power density of the scattered waves from the target and $P_{incident}$ is the power density of the incident wave [4]. This definition of RCS is usually referred to the monostatic or target RCS. This pertains to monostatic radars, meaning the radar receiver and transmitter are in

the same location, as opposed to a bistatic radar where they would be in different positions [5]. Bistatic radars have their own bistatic RCS, which is usually larger than monostatic RCS as with bistatic designs it is common to use multiple receivers, which means more scatter will be intercepted as compared to a monostatic design. Additionally, since RCS is dependent on angle, there will be a difference between monostatic and bistatic RCS [6]. The bistatic RCS equation can somewhat be derived from the monostatic, being

$$RCS_B \approx RCS_M \cdot cos\frac{\beta}{2} \tag{4}$$

where the bistatic RCS RCS_B equals the monostatic RCS RCS_M at the bisector of angle β, reduced in frequency by the factor of $\cos\frac{\beta}{2}$ [7]. Bistatic RCS is much more complex than monostatic, so monostatic RCS will be the focus of the next section.

With RCS defined, there are multiple ways to measure the RCS of an aircraft. Unlike simple objects, an aircraft is more difficult to measure due to its geometry. In short, the RCS of an aircraft is not as simple as a single amount measured in square meters, it is more of a range that changes based on certain parameters. Some examples can include the frequency of the radar and the angle of incidence of the aircraft. Tests are usually done inside within an anechoic chamber, which is lined with radar-absorbent foam to ensure accuracy, or done outside on a radar range. The object is usually elevated by a low RCS object or suspended to simulate flight. The resulting measurement is usually presented as a diagram, as seen in Fig. 2. Some of the most common methods to measure RCS are geometric optics (GO), physical optics (PO), and the method of moments (MoM).

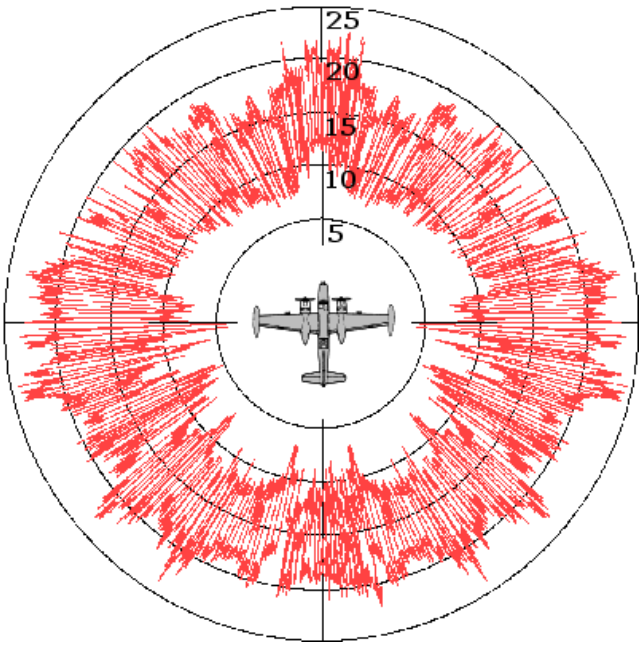

Fig. 2 RCS diagram of an A-26 Invader, notice the difference in RCS when measured from different directions

3. Methods & Technical Models

For simple objects, one method is usually enough to solve for the RCS. However, since an aircraft is composed of multiple shapes with multiple edges, a combination of methods is usually used to fully understand the RCS of aircraft. No one method is usually used for the entire aircraft, as different methods excel at different parts of the aircraft and so a combination is required. Additionally, multiple radar wavelengths would be tested to ensure low observability across a variety of wavelengths. All of the aforementioned methods for solving for the RCS of objects will be expanded upon in further detail here individually.

3.1. Geometric Optics (GO)

Geometric Optics is a simple method used to approximate the RCS of simple, large objects. In aircraft, this usually means the wings or the fuselage. As it is an approximation, it is only somewhat accurate and is usually supplemented by another method. GO is only valid when the size of the object is much, much larger than the wavelength of the wave tested (λ), as it assumes that all waves instead travel as rays. The main goal of GO is to identify specular points or reflections, which is an area where the incident radar wave would reflect directly backwards to the receiver, assuming that the radar is monostatic. In this case, the angle of incidence (θ_i) equals the angle of reflection (θ_r), being $\theta_i = \theta_r$. Next, the effective area of reflection must be calculated using the equation

$$A_{eff} = A \cdot \cos(\theta_i) \tag{5}$$

where the effective area A_{eff} equals area A multiplied by the cosine of θ_i to account for areas where the surface is not directly perpendicular with the wave. θ_i for perpendicular flat surfaces would be 0 degrees, however for curved surfaces it can vary. Curved surfaces in general are more difficult to calculate, and so the effective area is either usually approximated as flat, or will be integrated for larger surface considerations using the equation

$$A_{eff} = \int_S \cos(\theta_i) dA \tag{6}$$

where S is the surface area, and dA is an infinitesimal area element on the surface. The effective area is directly equal to the RCS of the object [8]. The major limitation of the method is that it is incapable of accounting for diffraction or wave interactions at the corners and edges of objects, which is why GO is usually used in conjunction with other methods.

3.2. Physical Optics (PO)

Physical Optics is another approximation method that improves upon Geometric Optics by treating electromagnetic waves as they are, which accounts for properties that waves would have, such as diffraction. This means that as opposed to GO, it is a bit more accurate in terms of the measurement. It also serves as a basis for the Method of Moments [9]. While there are multiple ways to calculate this method, one will be described. Another method to use PO can be found in reference 9. To use PO, it is assumed that the target is perfectly conductive, and that the target is in the far field of the radar, which means the waves are more predictable as opposed to the near field, where the waves are much more complex. Additionally, a tangent plane approximation is applied to the target to simply the calculation. First, the general form of the Stratton-Chu Integral Equation, being

$$E_{scattered}(r) = \frac{j\omega\mu}{4\pi} \int_S \left[n \cdot (J(r') \cdot \frac{e^{-jk|r-r'|}}{|r-r'|}) \right] dS' \tag{7}$$

where $E_{scattered}(r)$ is the scattered electric field at observation point r, $J(r')$ is the surface current density at surface point r', n being the surface normal vector at r', k being the angular wavenumber $k = \frac{2\pi}{\lambda}$ with a wavelength of λ, and dS' being the differential surface area element. The equation must then be modified to fit the far field. The modified and simplified equation becomes

$$E_{scattered}(r) = \frac{e^{-jkR}}{4\pi R} \int_S [n \cdot (J(r'))] \, dS' \tag{8}$$

for distance R between the radar and the target. Next the surface density J must be calculated via its relation to the incident electric field $E_{incident}$ assuming a perfectly conducting surface. By using the equation

$$J = \frac{E_{incident} \cdot n}{\eta} \tag{9}$$

where η is the impedance of free space $(\eta \approx 377\Omega)$. By substituting J into the previous equation, we can evaluate the integral over surface area S to find $E_{scattered}$ with the new equation

$$E_{scattered}(r) = \frac{e^{-jkR}}{4\pi R\eta} \int_S [n \cdot (E_{incident} \cdot n)]\, dS' \tag{10}$$

which gives us $E_{scattered}$. By plugging the result and $E_{incident}$ back into the RCS equation for electric field density (2), we can get the final RCS of the object [9]. Again, this method is similar to GO where it is good for large bodies, but still cannot give values for edges. Additionally, it is still an approximation, and so to find a concrete value another method must be used.

3.3. Method of Moments (MoM)

While being the most accurate of the three methods, as it gives an exact value, it is also the most challenging to calculate by hand. Unlike the two other methods, MoM can handle arbitrary geometries, which makes it the preferred method when measuring aircraft. However, it is incredibly complex, which is why it is usually done by computers using software programs. It begins by generating a surface patch model of surface S', essentially meaning that the surface is divided into N pieces, called patches. Each patch should be around 1/10 of a wavelength in size. Basis functions $\vec{B}_n$ should be used to approximate $\vec{J}$, the current density, for each segment. $\vec{J}$ is equivalent to

$$\vec{J}(\vec{r}) = \sum_{n=1}^{N} I_n \vec{B}_n(\vec{r}) \tag{11}$$

Next, Maxwell's equations are transformed via the Green's theorem which becomes the equations

$$\vec{E}_{scattered} = \oiint_{S'} \left[+i\omega\mu(\hat{n} \times \vec{H})\psi + (\hat{n} \times \vec{E})x\vec{\nabla}\psi + (\hat{n} \cdot \vec{E})\vec{\nabla}\psi\right] dS' \tag{12}$$

and the equation

$$\vec{H}_{scattered} = \oiint_{S'} \left[+i\omega\varepsilon(\hat{n} \times \vec{E})\psi - (\hat{n} \times \vec{H})x\vec{\nabla}\psi - (\hat{n} \cdot \vec{H})\vec{\nabla}\psi\right] dS' \tag{13}$$

in which

$$\psi = \left[\frac{e^{+ikR}}{4\pi R}\right] \qquad R = |r - r'| \tag{14}$$

where the Green's function in free space is a spherical wave that falls off as $\frac{1}{R}$. It is important to remember that for the electric field, $\vec{E} = \vec{E}_{incident} + \vec{E}_{scattered}$ and for the magnetic field, $\vec{H} = \vec{H}_{incident} + \vec{H}_{scattered}$. The previous equations can be directly used to calculate the scattered field, but is more complex and so will be altered into a form of the Electric Field Integral Equation (EFIE) and Magnetic Field Integration Equation (MFIE), which assumes a perfectly conducting surface. The equations then become

$$\vec{E}_{scattered} = \oiint_{S'} \left[+i\omega\mu(\hat{n} \times \vec{H})\psi + (\hat{n} \cdot \vec{E})\vec{\nabla}\psi\right] dS' = \oiint_{S'} \left[+i\omega\mu J\psi + \frac{1}{\varepsilon}\rho\nabla\psi\right] dS' \tag{15}$$

and

$$\vec{H}_{scattered} = \oiint_{S'} (\hat{n} \times \vec{H}) \times \nabla\psi dS' = \oiint_{S'} \vec{J} \times \nabla\psi dS' \tag{16}$$

These equations are difficult to solve, so by applying the boundaries of Maxwell's equations and the continuity equation for free space, the new equations of

$$\hat{n} \times \vec{E}_{incident} = -\hat{n} \times \vec{E}_{scattered} = \hat{n} \times \oiint_{S'} \left[+i\omega\mu\vec{J}\psi + \frac{+i}{\omega\varepsilon}\nabla \cdot \vec{J}\nabla\psi \right] dS' \tag{17}$$

$$\hat{n} \times \vec{H}_{incident} = \frac{\vec{J}}{2} - \hat{n} \times \oiint_{S'} \vec{J} \times \nabla\psi dS' \tag{18}$$

are created, with the continuity equation being that $\nabla \cdot J + \frac{\partial \rho}{\partial t} = 0$. Next, the magnetic field operator of $L_H(\vec{J})$ is defined, being the altered MFIE previously defined, as the equation

$$L_H(\vec{J}) \equiv \frac{\vec{J}}{2} - \hat{n} \times \oiint_{S'} \vec{J} \times \nabla\psi dS' \tag{19}$$

By inserting the series expansion of currents created at the very beginning and bringing the sum out of the operator, the equation becomes

$$L_H(\vec{J}) = \sum_{n=1}^{N} I_n L_H \left(\vec{B}_n(\vec{r}) \right) = \hat{n} \times \vec{H}_{incident} \tag{20}$$

Multiplying this with a weighting vector of $\vec{W}_m$, where $m = 1, 2, 3, \ldots N$, and integrating over the surface, we get the equation

$$\oiint_S \left[\vec{W}(\vec{r}) \cdot \left(n \times \vec{H}_{incident} \right) \right] dS - \sum_{n=1}^{N} I_n i\omega\mu \oiint_{S'} \oiint_S \vec{W}_m \cdot L \left(\vec{B}_n(\vec{r}) \right) dS' dS = 0 \tag{21}$$

The preferred method for solving this integral for I_n is Galerkin's Method, where $\vec{W}_m = \vec{B}_m(\vec{r})$, which means it can be substituted into the equation. Next, the Matrix Z_{mn} and the vector V_m is formed using the integrals

$$Z_{mn} = \oiint_{S'} \oiint_S \left[\vec{B}_m(\vec{r}) \cdot L \left(\vec{B}_n(\vec{r}) \right) \right] dS' dS \tag{22}$$

$$V_m = \oiint_S \vec{B}_m(\vec{r}) \cdot \left[n \times \vec{H}_{incident} \right] dS \tag{23}$$

Finally, to solve for I_n the linear system $ZI = V$ is used, and to solve for I the matrix of Z is inverted, making $I = Z^{-1}V$. With I_n calculated, it can be plugged back into the first equation for $\vec{J}$, which can then be used to find $\vec{E}_{scattered}$. Finally, plugging everything into equation (2) gives the exact RCS of the object [8].

4. Experiments & Model Evaluation

Within the methods of exact RCS calculations, there is little difference when comparing methods. While comparing approximations, like PO, against exact measurements, like MoM, will definitely show a difference, comparing exact methods shows only a few decibels of difference in RCS, as seen in this report. When comparing results from MoM and another exact method, the Finite Element Method (FEM), the report concludes that "The agreement between the two sets of results has generally been within a few decibels where the RCS was large enough to matter. Since default meshing and default convergence parameters were used for most of the HFSS calculations, the quality of the agreement must be regarded as satisfactory. For the one case where the default parameters were not adequate, the RCS was sufficiently low enough to not be of concern" [10], meaning that the methods were close enough for either or to be used. However, the report mainly focuses on UAVs,

which are much cheaper and have looser parameters compared to manned aircraft. When considering that factor, the slight discrepancy should be considered, and specific methods may be better than others for measuring the RCS of an aircraft.

5. Conclusion

The future of air combat will be dominated by radar. With longer-ranged munitions like the AIM-174B being fielded, the engagement distance of the future will only extend. A combination of manned and unmanned systems will dominate the future air war, using sensor fusion technologies along with ever-powerful radar to find the target before the target finds them. It is therefore imperative that future sixth-generation designs and beyond, be they manned or unmanned, possess as many low observable features as possible. This does not just apply to aircraft, as warships have been employing similar technologies as well. The *Zumwalt*-class destroyer is a good example of an albeit failed stealth warship design. However, low observability applies not just to radar visibility, but also covers other electronic detection methods such as infrared detaction. While camouflage is designed to obscure the object in the real space, LO aims to achieve the same in the electronic space. While active camouflage may only exist in science fiction, in the modern battlefield, low observability is the closest possible alternative.

References

[1] Manikas, A. (2020, January). *EE3-27: Principles of classical and modern radar - radar cross section (RCS) & radar clutter*. https://skynet.ee.ic.ac.uk/notes/Radar_4_RCS.pdf

[2] Anritsu. (2011, June). *Measuring radar cross section with handheld VMAs*. Defense Tech Briefs. https://dl.cdn-anritsu.com/en-us/test-measurement/files/Brochures-Datasheets-Catalogs/ Articles/ 11410-00620A.pdf

[3] Borkar, V., Ghosh, A., Singh, R., & Chourasia, N. (2010). Radar cross-section measurement techniques. *Defence Science Journal*, *60*(2), 204-212. https://doi.org/10.14429/dsj.60.341

[4] Mahafza, B. R. (2000). *Radar systems analysis and design using MATLAB*. CRC Press

[5] Jenn, D. (2010). *EC4630 Radar and laser cross section*. Naval Postgraduate School. https://faculty.nps.edu/ jenn/EC4630/RCSintroductionV2.pdf

[6] Johnsen, T., & Olsen, K. E. (2006). Bi- and multistatic radar. *Advanced Radar Signal and Data Processing*, 4-1 - 4-34. https://www.sto.nato.int/publications/STO%20Educational%20Notes/Forms/Educational%20Notes%20Document%20Set/docsethomepage.aspx?ID=2067&FolderCTID=0x0120D5200078F9E87043356C409A0D30823AFA16F60300099FA443AE6E08499A57A0FBE0134F20&List=44a8f49d-e481-458a-91b4-212a9605bd9e&RootFolder=https://www.sto.nato.int/publications/STO%20Educational%20Notes/RTO-EN-SET-086

[7] Manikas, A. (2020, February). *EE3-27: principles of classical and modern radar - bistatic radar*. https://skynet.ee.ic.ac.uk/notes/Radar_7_Bistatic_Radar.pdf

[8] O'Donnell, R. M. (2010, January 1). *Radar systems engineering lecture 7 part 2 radar cross section* [PDF]. radar-course.org. http://radar-course.org/Radar%202010%20PDFs/Radar%202009%20A_7% 20Radar%20Cross%20Section%202.pdf

[9] Williams, L. L. (1999, January). *Physical optics theory of radar cross section*. Konfluence Research Institute. https://konfluence.org/media/metrad/PO_RCS.pdf

[10] Spurgeon, W. A. (2010). *Rcs Predictions from a Method of Moments and a Finite-Element Code for Several Targets*. GovInfo | U.S. Government Publishing Office. https://www.govinfo.gov/app/details/GOVPUB-D101-PURL-gpo1559.